UDC 519.61:621.313.13
Original scientific paper
Received: 31.07.2002.

Modelling magnetic characteristics of steel secondary of a linear induction motor

Hasan Kürüm[(1)], **Hüseyin Altun**[(2)] and **Hanifi Guldemir**[(3)]
[(1)]Department of Electrical and Electronics Engineering, Firat University, 23119 Elazig, TURKEY
[(2)]Technical Education Faculty, Department of Electrical Education, Firat University, 23119 Elazig, TURKEY
[(3)]Technical Education Faculty, Department of Electronics and Computer Science, Firat University,
23119 Elazig, TURKEY, e-mail: hkurum@firat.edu.tr; hguldemir@firat.edu.tr

SUMMARY

In this paper, electrical and magnetic characteristics of the secondary material of a constructed model linear induction motor (LIM) with solid iron secondary disc have been experimentally obtained. For obtaining the magnetic characteristics of the secondary material a torus has been constructed from the same material on which a toroidal coil has been wound. The B-H characteristics of this torus has been determined experimentally. For consideration the magnetic characteristics of this secondary material in the calculations, a mathematical B-H characteristic has been modeled by using those results obtained from experiment.

***Key words**: magnetic conductivity, magnetic reluctivity, B-H characteristic, linear induction motor.*

1. MODEL LINEAR INDUCTION MOTOR

In this paper, the linear induction motor on which the experimental work has been carried out is double sided. In structural meaning the stators on both sides have the same characteristics. The laminated sheet iron core arranged on the body of each stator has been manufactured by pressing 434 pieces of *0.3 mm* thick and treated siliceous sheet iron. The iron core of each stator is *54 cm* long, *13 cm* wide, and *4 cm* high including the slot structure of the stator. The depth is *18 mm* and the width is *8 mm* of each stator slot. The thickness of the stator tooth is *6 mm.* On one side of each sheet iron 36 slots for the stator winding and on the other side 3 number of swallow tails for mounting the iron core on the stator body exist. The body on which the stator iron core is mounted has been constructed from casting aluminum. Three phase stator winding has been wound to constitute 4 magnetic poles using non-equal pitch winding technique. The diameter of the winiding conductor is 3*0,65 mm. Since each sub-coil consists of 22 winding pairs, there exist in each stator slot 44 winding pairs.

Instead of extending the secondary (rotor) and make the primary (stator) moving, the primary can be held stationary and the secondary constructed of a rotary conductive disc. In this study, the model linear asynchronous has been constructed of the latter type, in order to save space and enable continuous operation. The secondary sheet iron disc is *1.3 cm* thick and has *120 cm* diameter. The constructed LIM is seen in Figure 1 [8].

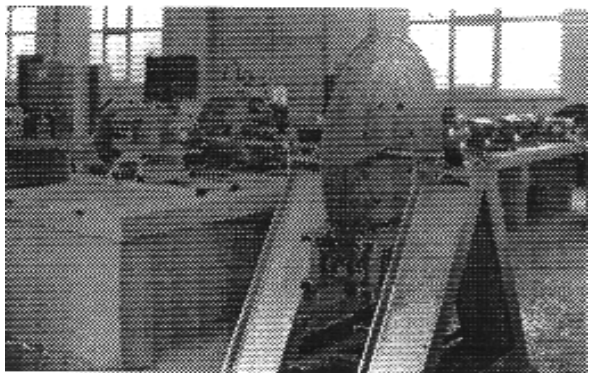

Fig. 1 The aspect of the LIM used in the experimental work

2. MAGNETIC CHARACTERISTIC OF THE SECONDARY MATERIAL

A torus has been constructed from the same material of the secondary to obtain its magnetic characteristic. The inner diameter of the torus is *10 cm* the outer diameter is *26.5 cm*, and the thickness of the torus is *12 mm*.

A primary and a secondary windings have been wound on the torus using the same copper conductor. The diameter of the cooper conductor used for the winding is *0.65 mm*. The toroidal winding consists of three main layers. On the first layer 300 turns, on the second layer 275 turns, and on the third layer 100 turns have been wound. Above values have been obtained from a developed computer program which takes into account the magnetic saturation for determining approximately the size and number of turns of the toroidal system. The experiment has been realized under *50 Hz*, the mains frequency. The primary current has been increased from *0 A* to *9 A*. For *9-ampere* primary current, the secondary voltage has been measured as *150 volt*. The toroidal system used in the experiment has been replaced in a container filled with transformer oil. Therefore, cooling the coils in the system has been provided appropriately. Connection scheme of the experiment is seen in Figure 2.

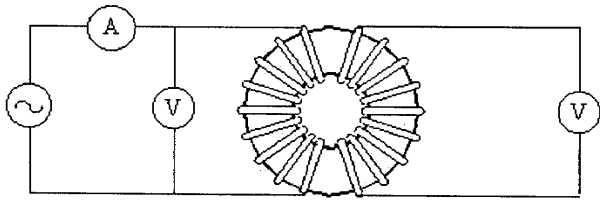

Fig. 2 Connection scheme of the experiment

The Table 1 tabulates the induced secondary voltages against the primary currents. Using the experimental results some magnetic quantities in the toroidal call be calculated from the following expressions:

$$e = 4.44 * n * F * \phi \tag{1}$$

$$\phi = \frac{e}{4.44 * N * f} \tag{2}$$

$$B = \frac{\phi}{S} \tag{3}$$

$$H = \frac{N * I}{L} \tag{4}$$

where e is the voltage induced in the secondary *[V]*, N is the number of turns, f is frequency *[Hz]*, B is magnetic induction *[T]*, H is magnetic field intensity *[At/m]*, and L is the mean length of the magnetic flux *[m]*. The *B-H* curve using *L=0.573 m* and *f=50 Hz* is shown in Figure 3.

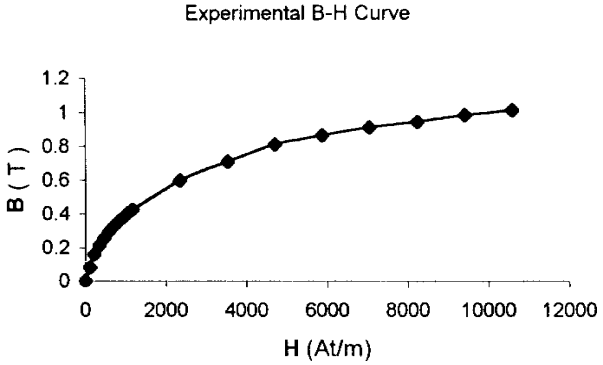

Fig. 3 The experimentally obtained B-H curve

3. MATHEMATICAL EXPRESSION OF THE EXPERIMENTAL B-H VALUES

For considering the magnetic saturation in numerical analysis of magnetic field problems, determining a mathematical expression related to the magnetizing curve is inevitable. In the analysis using finite element and finite difference methods the equation coefficients are the function of the magnetic permeability [1, 2, 7, 10, 12, 13, 14. Therefore it is necessary to express the magnetic variations mathematically.

3.1 Expression of the experimental results with one-term Frohlich equation

Neglecting the hysteresis losses and using one-term Frohlich equation the experimental results of *B-H* values can be formulated mathematically:

$$B(H) = \frac{B_s * H}{C_1 + C_2 * H} + \mu_0 * H \tag{5}$$

where μ_0 is the magnetic permeability of free space, and C_1 and C_2 are constant coefficients. In Frohlich equation B_s is the point value of magnetic induction

Table 1 Voltage induced in the secondary versus the primary current

Eksperimental Results:																			
Primary Current (Ampere)	*0*	*0.1*	*0.2*	*0.3*	*0.4*	*0.5*	*0.6*	*0.7*	*0.8*	*0.9*	*1*	*2*	*3*	*4*	*5*	*6*	*7*	*8*	*9*
Secondary Voltage (Volt)	*0*	*18.5*	*24*	*32*	*38.5*	*44*	*48.2*	*52.5*	*56.5*	*60*	*67*	*89*	*105*	*120*	*128*	*135*	*140*	*146*	*150*

near the saturation point and the magnetizing curve becomes linear. This value has been determined to be *0.94 Tesla* for the material used in the experiment. For calculating the coefficients C_1 and C_2 using the least squares approach the Eqs. (6) and (7) are derived from Eq. (5) dividing both sides of Eq. (5) by B_s*H and defining BR as:

$$BR = \frac{B_s * H}{B(H) - \mu_0 * H} \tag{6}$$

$$BR = C_1 + C_2 * H \tag{7}$$

Using the least squares approach the coefficients C_1 and C_2 are calculated from the following equation:

$$\begin{bmatrix} n & \sum_{i=1}^{n} H_i \\ \sum_{i=1}^{n} H_i & \sum_{i=1}^{n} H_1^2 \end{bmatrix} * \begin{bmatrix} C_1 \\ C_2 \end{bmatrix} = \begin{bmatrix} \sum_{i=1}^{n} BR_i \\ \sum_{i=1}^{n} BR_i * H \end{bmatrix} \tag{8}$$

Using the experimental results the coefficients C_1 and C_2 are found to be *1332,294* and *0,8956* respectively. Variations of the experimental values and values obtained from Frohlich's equation are seen in Figure 4.

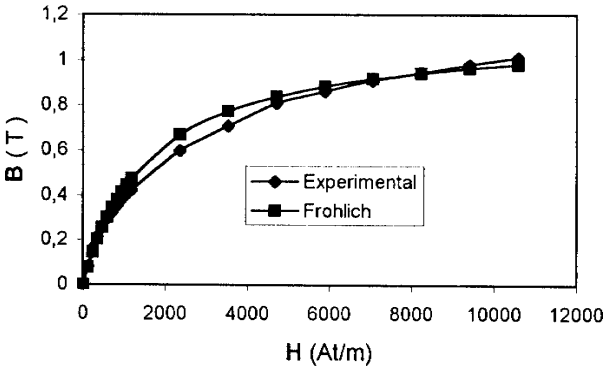

Fig. 4 Variation of experimental and B-H values obtained from Frohlich's equation

In the calculations magnetic permeability and magnetic resistivity need to be known [3, 4, 5, 6, 10, 14]. Taking the derivative of Frohlich expression with respect to H, the $\mu(H)$ and $v(H)$ are found to be:

$$\mu(H) = \frac{dB}{dH} = \frac{C_1 * B_s}{(C_1 + C_2 H)^2} + \mu_0 \tag{9}$$

$$v(H) = \frac{1}{\mu(H)} \tag{10}$$

3.2 Expression of the experimental results with two-term Frohlich equation

Since there is an error of *12%* between real experimental values and the values obtained from Frohlich's equation in Eq. (5), the same experimental values have been formulated mathematically using two-term Frohlich equation. Accordingly, part of the curve shown in Figure 4 where the magnetic induction becomes linear can be represented as:

$$B_1 = \frac{H}{a_1 + b_1 * H} \quad , \quad (B \le B_s) \tag{11}$$

and the remaining of the curve can be represented as:

$$B_2 = B_s + \frac{H - H_s}{a_2 + b_2 (H - H_s)} \quad , \quad (B \ge B_s) \tag{12}$$

The coefficients of these equations can be determined as presented below as well as mentioned in Subsection 3.1 by using the least squares approach.

From Eq. (11):

$$v = \frac{H}{B} = \frac{a_1}{1 - B * b_1} \tag{13}$$

can be obtained.

In Figure 5 the variation is approximately linear until the point P_d. If the reluctivity at this point is shown by v_d, then:

$$v_d = \frac{H_d}{B_d} = \frac{a_1}{1 - b_1 * B_d} \tag{14}$$

is obtained. At the point P_s:

$$B_s = \frac{H_s}{1 - b_1 * H_s} \tag{15}$$

is defined.

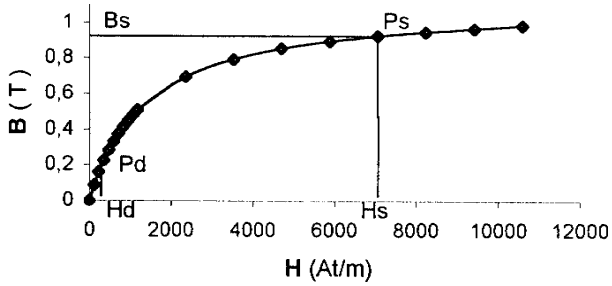

Fig. 5 Variation of the experimental results using two-term Frohlich equation

Substituting Eqs. (14) and (15) in Eqs. (11) through (13) the coefficients a_1 and b_1 can be expressed respectively as:

$$\begin{aligned} a_1 &= v_d - \frac{H_s - v_d * B_s}{B_s (H_s - v_d * B_d)} * v_d * B_d \\ H_d &= v_d * B_d \end{aligned} \tag{16}$$

$$a_1 = v_d - \frac{H_d * (H_s - v_d * B_s)}{B_s (H_s - H_d)} \tag{17}$$

$$b_1 = \frac{H_s * v_d * B_s}{B_s (H_s - H_d)} \tag{18}$$

For determining the coefficients of the equation which represents the second region, at the point, $P_s(H_s,B_s)$ values and derivative of Eqs. (11) and (12) should be equal. Therefore at the point where H=H_s:

$$B_1 = B_2 \quad ve \quad \frac{dB_1}{dH} = \frac{dB_2}{dH} \tag{19}$$

should be satisfied. If the solution which satisfies these conditions is reached, then the coefficients a_2 and b_2 can be found as:

$$a_2 = \frac{(a_1 + b_1 * H_s)^2}{a_1} \tag{20}$$

$$b_2 = \frac{-a_2 + \sqrt{\frac{a_2}{\mu_{ss}}}}{H_{ss} - H_s} \tag{21}$$

The slope of the curve beginning from where the curve becomes linear in the second region is given as:

$$\frac{dB_2}{dH_{ss}} = \mu_{ss} = \frac{a_2}{(a_2 + b_2(H_{ss} - H_s))^2} \tag{22}$$

For the curve used in this work some values have been found to be B_s=*0.9437 T*, H_s=*8241.758 At/m*, B_d=*0.161 T*, H_d=*235.47 At/m*. The best value for H_{ss}, has been taken as $3*10^5$ *At/m* after some numerical trials. By using these values the coefficients have been found to be a_1=*1241.677*, b_1=*0.909*, a_2=*61427.53*, *b2=5.47E-01*. The curve obtained using these coefficients, variation of the experimental results, and variation of the results from one-term Frohlich equation on the same scale are seen in Figure 6.

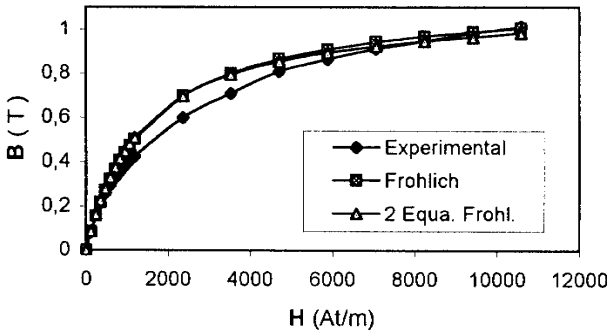

Fig. 6 All variations on the same scale

In the above equations, values of H_d and B_d are directly read from the experimental curve. However, values of B_s and H_s can be read directly from the experimental curve as well as can be determined by some numerical trials to give the best curve.

In the calculations magnetic reluctivity need to be known [9, 11]. If the derivative of Frohlich expression is taken for *H*, then values of *v(H)*, for the first and second region, can be written as in the following equations:

$$v_1 = \frac{a_1}{1 - b_1 * B} \quad , \quad (B \le B_s) \tag{23}$$

$$v_2 = \frac{(a_2 - b_2 H_s)(B - B_s) + H_s}{B(1 - b_2(B - B_s))} \, , (B \ge B_s) \tag{24}$$

4. DETERMINATION RESISTANCE OF THE SECONDARY MATERIAL

ST-37 steel material which is used in the secondary has been used for the electrical resistance measurement. A bar has been cut from this material which has *12*15 mm*^{2} cross section and *500 mm* length. The resistance of this material has been determined via a dc test. The Ammeter-Voltmeter method has been used in measuring the resistance of this material.

In measuring the resistance, to keep the error minimum due to this method the ammeter has been connected before the voltmeter. For removing the effects of some other resistances due to the measurement equipment sufficiently thick copper connectors have been used. The joints between these connectors and the material have been constituted using a suitable welding technique. The voltmeter and ammeter used in the experiment have *1%* measurement error.

In the dc test for obtaining the value of the resistance, first *5 Ampere* and then *10 Ampere* have flown in the conductors. From the voltmeter *4.3 mV* and *8.6 mV* have been measured respectively for these two different currents. From these values the electrical resistance of the bar has been calculated as:

$$R = \frac{U}{I} = \frac{8.6 * 10^{-3}}{10} = 0.00086\,\Omega$$

By replacing the value of the material cross section, S=*0.012*0.015=1.8*10*$^{-1}$ m^2 , in the expression below resitivity of the material can be found:

$$R = \frac{L}{\rho * S} = \frac{0.5}{\rho * 1.8 * 10^{-4}} = 0.00086\,\Omega$$

$$\rho = 3229974.16 \frac{1}{\Omega\ m}$$

$$\frac{1}{\rho} = 3.096 * 10^{-3}\,\Omega\ m$$

5. CONCLUSION

In the calculations of the LIM model using the finite element method and one-dimensional direct analysis methods, considerable differences between the experimental and the theoretical results have been observed to be occurr. There are many reasons that cause these differences. Two of these reasons are due to the usage of constant magnetic reluctivity and the electrical conductivity values for cast iron or cast steel given in the catalogues. As it can be seen from the experimental results shown in Figure 3, the *B-H* curve of the steel material, ST-37 is nonlinear. Accordingly, it is not possible for the magnetic reluctivity to have a constant value. Therefore, taking the magnetic reluctivity constant some errors will ocurr in the theoretical calculations. Differences between the

theoretical and experimental results will decrease provided that the proposed mathematical model of this work is used.

6. REFERENCES

[1] H. Alwash and J.A.H. Al-Rikabi, Finite element analysis of linear induction machines, *Proc. IEE*, Vol. 126, No. 7, pp. 677-682, 1979.

[2] M.V.K. Chari and P.D. Silvester, *Finite Element in Electrical and Magnetic Field Problems*, John Wiley and Sons, New York. 1984.

[3] M.V.K. Chari, Finite element analysis of nonlinear magnetic fields in electric machines, Ph.D. Thesis, Mc Gill University, Montreal, Quebee, 1970.

[4] M.V.K. Chari and P.D. Silvester, *Finite Element in Electrical and Magnetic Field Problems*, John Wiley and Sons, New York. 1984

[5] J.F. Eastam, M.J. Balchin and D. Dodger, Measurement and calculation of rotor-core flux densititics in axial flux linear induction motors, *Proc. IEE*, Vol. 128, No. 6, 1981.

[6] J. Faiz and H. Jafari, Accurate modeling of single-sided linear induction motor considers end effect and equivalent thickness, *IEEE Transactions on Magnetics*, Vol. 36, No. 5, pp. 3785-3789, 2000.

[7] H. Kürüm and A. Shobair, Double-sided linear induction motor with a rotary solid steel-secondary disc, *International Journal for Engineering Modelling*, Vol. 13, No. 3-4, pp. 107-109, 2000.

[8] H. Kürüm, Finite element analysis of double-sided linear induction motors, Ph.D. Thesis, University of Firat, Elazig, 1990.

[9] M. Poloujadoff , *The Theory of Linear Induction Machines*, Oxford University Press Inc., New York, U.S.A., 1980.

[10] S.A. Nasar, Certain Approaches to The Analysis of Singel-Sided Linear Induction Motors, *Proc. IEE*, Vol. 120, No. 4, pp. 477-483, 1973.

[11] S.A. Nasar and I. Boldea, *Linear Motion Electric Machines*, New York, Wiley, 1976.

[12] J. Penman, B.J. Chalmers, A.M.A. Kamar and R.N. Tuncay, The performance of solid steel secondary linear induction element analysis of linear induction machine, *IEEE Transaction on Power Apparatus and Systems*, Vol. 100, No. 6, pp. 2927- 2935, 1981.

[13] R.M. Pai, I. Boldea and S.A. Nasar, Complete equivalent circuit of a linear induction motor with shett secondary, *IEEE Transactions on Magnetics*, Vol. 24, No. 1, 1988.

[14] T. Yamaguchi, Y. Kawase, M. Yoshida, Y. Saito and Y. Ohdachi, 3-D finite element analysis of a linear induction motor, *IEEE Transactions on Magnetics*, Vol. 37, No. 5, pp. 3668-3671, 2001.

MODELIRANJE MAGNETSKIH KARAKTERISTIKA ČELIKA SEKUNDARNOG NAMOTA LINEARNOG INDUKCIJSKOG MOTORA

SAŽETAK

U ovom radu eksperimentalno su dobivene električne i magnetske karakteristike materijala sekundarnog namota konstruiranog modela linearnog indukcijskog motora (LIM) s krutim željeznim sekundarnim diskom. Da bi se dobile magnetske karakteristike sekundarnog materijala konstruiran je torus od istog materijala oko kojega je bila namotana toroidalna zavojnica. B-H karakteristike ovog torusa određene su eksperimentalno. Da bi se mogle računski iskazati magnetske karakteristike ovog sekundarnog materijala, modelirala se matematička B-H karakteristika koristeći rezultate dobivene eksperimentom.

***Ključne riječi**: magnetska provodljivost, magnetska otpornost, B-H karakteristike, linearni indukcijski motor.*